Vibrational Spectroscopy 61 (2012) 144–150

Contents lists available at SciVerse ScienceDirect

Vibrational Spectroscopy

journal homepage: www.elsevier.com/locate/vibspec

Far-infrared spectroscopy analysis of linear and cyclic peptides, and lysozyme

Tao Ding[a], Anton P.J. Middelberg[a], Thomas Huber[b], Robert J. Falconer[c,*]

[a] Australian Institute for Bioengineering and Nanotechnology, The University of Queensland, Brisbane, QLD, Australia
[b] Research School of Chemistry, Australian National University, Canberra, ACT, Australia
[c] Department of Chemical & Biological Engineering, ChELSI Institute, University of Sheffield, Sheffield, England, United Kingdom

ARTICLE INFO

Article history:
Received 14 November 2011
Received in revised form 25 February 2012
Accepted 28 February 2012
Available online 7 March 2012

Keywords:
Terahertz
Far-infrared
Synchrotron
Molecular dynamics
VDOS

ABSTRACT

The far-infrared spectra of lysozyme, alanine-rich peptides and small cyclic helical peptides were studied. Both lysozyme and the alanine-rich peptides had a dome in the spectral background centred on 180–220 cm^{-1} consistent with either structural collective modes or an ensemble of hydrogen bond vibrational modes associated with the peptide backbone. Molecular dynamics simulation of the alanine-rich peptide's infrared spectrum produced bands with similar positions to the experimental data and vibrational density of states simulation was able to attribute several of these bands to backbone and side chain vibrational modes. Evidence is presented that peaks at 333 and 375 cm^{-1} are associated with alpha-helices in lysozyme and the alanine-rich peptides, and the peak at 445 cm^{-1} is associated with beta-pleated sheet. Also, results suggest that peaks at 385, 402 and 470 cm^{-1} are associated with the secondary structure of the cyclic helical peptide KARAD. This supports the hypothesis the low energy vibrational modes between 300 and 500 cm^{-1} are diagnostic of the presence of secondary structures in (poly)peptides.

1. Introduction

Proteins are a fundamental component to life and are the centre of considerable research effort aiming to understand the physicochemical basis of their functionality. New methods of studying protein structure, conformational change and flexibility, and the interaction between proteins and water, are needed to better characterize biological function. The advent of Terahertz time domain spectroscopy (THz-TDS) in the 1990s provided a new technique for studying the absorbance spectra between the far-infrared and microwave wave numbers, and promised to allow low energy vibrations to be studied that were previously unobservable. New interest in this part of the spectrum also led to a reassessment of earlier far-infrared spectroscopy research that was undertaken in the 1960–1980 period as the THz-TDS and early far-infrared spectroscopy overlap between the wave number values of 20–150 cm^{-1}, making these complementary technologies over much of their respective bandwidths.

Early far-infrared spectroscopy research on peptides and proteins focused on simple compounds including polyamides or N-methylacetamide. The vibrational spectrum of N-methylacetamide is particularly informative as it the simplest molecule with a peptide bond so attribution of peaks to specific vibrational modes is simpler than for complex molecules. N-methylacetamide has an absorbance peak at 120 cm^{-1} that was assigned to intermolecular hydrogen bonding and a peak at 201 cm^{-1} assigned to C—N torsional vibration [1] although the N—H out-of-plane mode may also contribute to this peak [2]. Polyamides with known secondary structure were used to study the relationship between secondary structure and absorbance in the low wave number region. Studies of polyalanine found that alpha helical structures caused an absorbance peak centred on 370 cm^{-1} [3]. Beta-pleated sheet structures made using $(\text{L-Ala-Gly})_n$ and L-(Ala-Gly-Gly)_n showed absorbance centred on 235 and 440 cm^{-1} [4]. The early far-infrared spectra of proteins, however, had broad spectral features suggesting ensembles of vibrational modes that eluded meaningful interpretation [5]. More recently research on the amide VI band, the bending motion of the C=O group in the peptide backbone observed between 490 and 590 cm^{-1} has shown a correlation between the maxima's position and the secondary structure of a range of polyamino acids and proteins with a maxima around 525, 535 and 545 cm^{-1} being associated with alpha helices, random coils and beta sheets, respectively [6].

The introduction of THz-TDS (between 3 and 60 cm^{-1}) in the 1990s led to renewed investigation into the low energy vibrations in biomacromolecules [7,8]. THz-TDS of proteins invariably generated spectra with a monotonic rise in absorbance with increasing wave number but no discrete features such as peaks. Absorbance at these low wave number values has been linked to collective motions within the protein structure [9,10] which is of particular interest as it opens the possibility of studying protein dynamics. The internal bonding that holds protein structures in place is a

* Corresponding author. Tel.: +44 01142228253; fax: +44 01142227501.
E-mail address: r.j.falconer@sheffield.ac.uk (R.J. Falconer).

0924-2031/$ – see front matter © 2012 Elsevier B.V. All rights reserved.
doi:10.1016/j.vibspec.2012.02.020

combination of hydrogen bonding, exclusion of water from apolar residues (hydrophobic interaction), disulphide covalent bonding and possible electrostatic interaction and salt bridge formation, all of which are expected to contribute to the collective motions of a protein. This is consistent with the hypothesis raised by far-infrared research that suggested the broad peak below 300 cm^{-1} is dominated by intramolecular hydrogen bonding [11]. In vivo, most proteins are in an aqueous environment. The absorbance due to the hydration layer around proteins has to be taken into account as it can differ from the bulk water [12] and light scattering has to be taken into account for research into protein complexes [13,14]. Analysis of quaternary protein structures such as β-lactoglobulin fibrillar and globular gels likewise showed a monotonic relationship between absorbance and wave number values between 3 and 60 cm^{-1}, although globular gels which had higher apparent absorbance believed to be due to scattering of the photons by the soft globular protein structures [13]. Far-infrared spectroscopy of β-lactoglobulin gels and lysozyme fibrils gave mixed results with gelation causing minor changes to the spectrum and fibril formation causing light scattering [14,15]. The surprising observation for the lysozyme research was that the major structural change associated with denaturation of the lysozyme and formation of the intermolecular beta-sheets was not associated with a major change in the spectrum below 300 cm^{-1} indicating that interpretation of this part of the spectra is still problematic. Far-IR analysis of polyomavirus virus-like particles has more promise as the assembled particles gave a significantly different spectrum to the unassembled proteins. This could not be explained by light scattering but was associated with the self-assembly of the 50 nm diameter icosahedral viral protein structures [15].

There is increasing evidence that the solvation shell associated with a protein can be studied using THz-TDS and other spectroscopic techniques useful in this part of the electromagnetic spectrum [12,16,17]. Bulk water has a different absorbance to water in the solvation shell at wave number values between 15 and 80 cm^{-1}. This enables the thickness of the solvation shell to be estimated [12,16,17]. Analysis of peptide and protein in an aqueous environment absorbance spectrum is hampered by the absorbance of water in the Terahertz range. Even when frozen, the region between 150 and 300 cm^{-1} is lost due to water's OH···O connectivity band and between 650 and 1000 cm^{-1} is lost due to water's librational (swaying) band [18]. Lyophilization (freeze drying) removes water from the protein sample by sublimation and can result in less than 0.05 g/g residual water [19]. While dehydration can cause structural change in proteins it is an effective procedure to eliminate water from the analysis.

In this paper we applied far-infrared spectroscopy to study synthetic peptides and lysozyme with the goal of determining whether far-infrared analysis can provide useful information on peptide or protein structure. Three sets of analytes were studied; small pentameric helical cyclic (and non-cyclized) peptides with identical amino acid sequences, alanine-rich peptides with varying helicity and the small globular protein lysozyme. Molecular dynamic simulation and vibrational density of states simulation of the peptide AK17 were used to determine the contribution of the spectrum which was associated with the peptide backbone (which is directly related to the peptide's secondary structure) and that associated with the amino acid side chains.

2. Methods

The alanine-rich peptides were chemically synthesized with higher than 95% purity (Mimotopes, Clayton, Australia). The amino acid sequences of these peptides were AK17 (Ac-AKAAAAKAAAAKAAAAK-NH_2), AK10G (Ac-AKAAAAKAAGAKAAAAK-NH2) and AK9P (Ac-AKAAAAKAPAAKAAAAK-NH_2). The spectra of dry peptide were measured using pressed pellets containing 10 mg of peptide lyophilized powder mixed with 30 mg of Uvasol photometric grade polyethylene (Merck, Germany), pressed as 13 mm diameter discs, with 7 tonnes force for 3 min. Pellets were clamped into the cryostat cold finger ready for analysis. The KARAD peptides (the amino acid sequence being KARAD) were supplied by David Fairlie of the University of Queensland. Frozen aqueous samples of KARAD peptides were prepared and the far-infrared spectroscopic measurements were performed on the far-infrared and high resolution FTIR beamline at the Australian Synchrotron (Clayton, Victoria) as described previously [20].

Raman measurements were made on a Nicolet NXR FT-Raman spectrometer with NIR excitation at 1064 nm. Samples were measured as powder at room temperature. An InGaAs detector was used and the resolution was set to 2 cm^{-1} with 1024 scans over the range 3700–100 cm^{-1}.

Helicity was measured with a circular dichroism spectrometer (J-815, Jasco Tokyo, Japan). The peptides were dissolved in KF buffer at 100 μM prior to analysis. All measurements were conducted at 273 K. The helicity was estimated from the θ_{222} value [21].

Molecular dynamics simulations were performed with the GROMACS 3.3.2 package [22]. The peptide models were generated by Modeller as alpha-helical configuration [17]. The molecules were 'dissolved' in a simulation box of SPC [23] (single point charge, a 3-point model for water), the minimum distance between solute and the edge of box was set to 1.2 nm and the SPC (single point charge, a 3-point model for water) water model was used [24]. GROMOS 45A3 force field and NPT conditions (number of particles, system pressure and temperature (T = 273 K) held constant) were used to simulate each peptide. A twin-range cut-off scheme with 0.8 and 1.4 nm cut-off radii was applied. The integration time step was 2 fs and nonbonded interactions in the range between these radii were updated every fifth time step. Equilibrium simulations were performed for 6 ns prior to 1 ns of sampling period, in which the atomic trajectories were sampled every 20 fs. The simulated far-infrared absorbance spectrum was derived from the dipole time correlation function (TCF) [25].

Vibrational density of state (VDOS) simulation of the far-infrared absorbance spectrum reflects the overall dynamic of a peptide. It was obtained by the Fourier transformation of the auto-correlation of time dependent atomic velocity [26]. The same trajectories used to compute the dipole time correlation function were used calculating the VDOS of AK17, AK10G and AK9P, respectively.

3. Results and discussion

3.1. Optical analysis of alanine-rich peptides using far-infrared and Raman spectroscopy

The far-infrared spectra for AK17, AK10G and AK9P demonstrate that while the spectrum for AK10G is very similar to that for AK17, the spectrum of AK9P is significantly different having fewer discrete peaks and a different overall shape (Fig. 1). In solution the peptides have helicity measure by circular dichroism spectroscopy equal to 72.4% for AK17, 29.5% for AK10G and 0% for AK9P [17]. However, after freeze drying secondary structures of proteins are known to be modified [27]. In this case it is probable that the AK17 and AK10G both retained a structure dominated by alpha-helices but that AK9P formed a beta-sheet structure like polyalanine has in the solid state [4]. Raman IR spectroscopy of AK17 and AK9P of the Amide I peak (around 1660 cm^{-1}) showed a peak at 1657 cm^{-1} indicative of alpha-helice in AK17 and at 1665 cm^{-1} indicative of beta-sheet formation in AK9P (Fig. 2) [28,29]. Beta-sheet formation

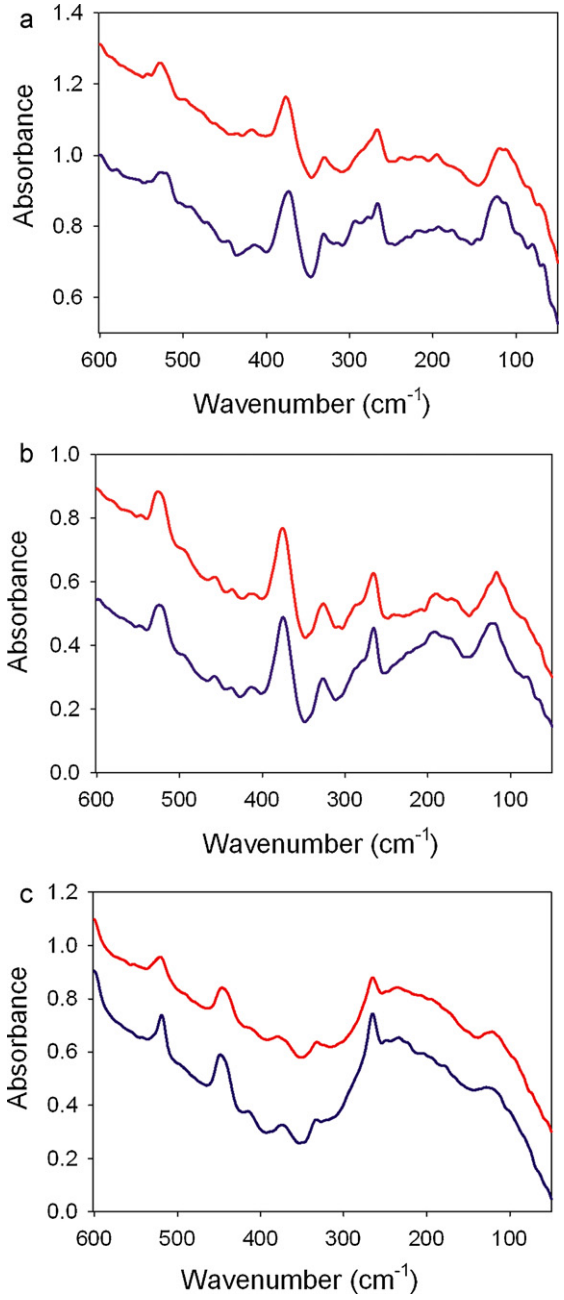

Fig. 1. Experimental far-infrared spectra (50–600 cm^{-1}) for lyophilized AK17, AK10G and AK9P (a, b, c, respectively). Spectra at 295 K (red) and 78 K (blue). Experimental spectra are offset vertically by 0.3 A.U. for clarity. (For interpretation of the references to color in this figure legend, the reader is referred to the web version of the article.)

in lyophilized AK9P is expected as it is observed in the closely related peptide polyalanine [4].

The far-infrared absorbance spectra for the peptides AK17 and AK10G are similar and relatively complex (see Fig. 1). The absorbance increases between 50 and 100 cm^{-1} to a peak at 120 cm^{-1}. A second minor peak is at 195 cm^{-1}. Next there is a peak with maxima at 265 cm^{-1} that has a shoulder seen in both AK17 and AK10G spectra. At 333 cm^{-1} there is a minor peak followed by a larger peak at 375 cm^{-1}. This is followed by evidence of minor peaks at 415 cm^{-1} and lastly a major peak at 520 cm^{-1}.

The infrared spectrum for AK9P is markedly different to AK17 and AK10G despite being chemically very similar (only differing in one amino acid out of 17). There are peaks at 120, 265, and

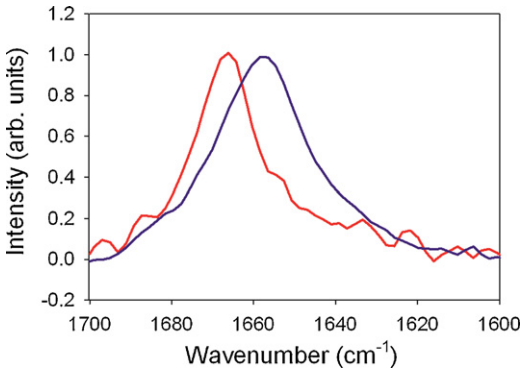

Fig. 2. Experimental Raman infrared spectra (1600–1700 cm^{-1}) of AK17 (blue) and AK9P (red) at 295 K. (For interpretation of the references to color in this figure legend, the reader is referred to the web version of the article.)

520 cm^{-1} that are seen in AK17 and AK10G. AK9P also has an additional peak at 445 cm^{-1}. The overall shape of the AK9P spectrum between 50 and 300 cm^{-1} is different indicating underlying differences between AK9P and AK17 collective modes.

The peak at 120 cm^{-1} displays a blue shift of around 3 cm^{-1} with reduced temperature (298 down to 78 K) which is consistent for all three peptide samples. This phenomenon was not observed for any other bands.

3.2. Molecular dynamic simulation of alanine-rich peptide far-infrared spectra

The simulated far-infrared absorbance spectrum derived from the dipole time correlation function gives the whole infrared spectrum of a molecule giving the band positions, the band intensities and the band shapes, through the Fourier transform of a time correlation function. It relies on the hypothesis of linear response theory, that the perturbation on the absorbing molecular system from the applied electric external field is small [30]. The far-infrared absorbance spectrum of AK17 was simulated as a structure dominated by an alpha-helical secondary rigid structure. The simulation was carried out at 273 K as it was experimentally observed that peak positions do not shift significantly at temperatures between 78 and 298 K, and the force fields used in the molecular simulations are parameterized to be most accurate at 273 K.

The wave number values of the bands in the simulated IR spectrum of AK17 are similar to those for the experimental peaks (Fig. 1a and 3, and Table 1). We propose that the simulated band at ~100 cm^{-1} corresponds to the actual band at 120 cm^{-1}, the simulated band at ~200 cm^{-1} corresponds to the actual maxima at 195 cm^{-1}, the three small simulated bands between 250 and

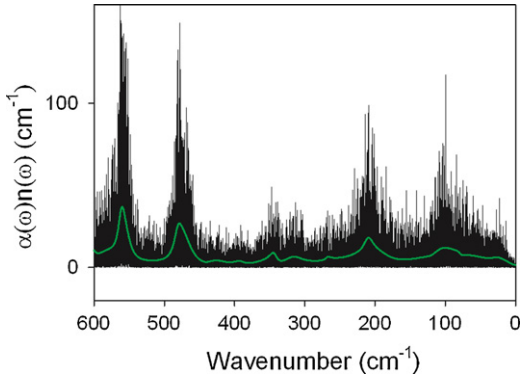

Fig. 3. Molecular dynamics simulation of the far-infrared spectrum of AK17 (0–600 cm^{-1}) compared with the experimental spectrum.

Table 1
Bands on AK17 (and AK9P).

Exp. IR bands	Calc. IR bands	Present in AK9P	VDOS peptide backbone	VDOS side chain	VDOS hydrogen	Interpretation
120 cm^{-1}	100 cm^{-1}	+	+	+	–	Uncertain but not hydrogen bonding
195 cm^{-1}	200 cm^{-1}	–	+	–	+	Hydrogen bonding of the peptide backbone
265 cm^{-1}	270 cm^{-1}	+	na	na	na	Uncertain
333 cm^{-1}	320 cm^{-1}	–	+	–	–	Alpha helix
375 cm^{-1}	340 cm^{-1}	–	+	+	–	Alpha helix (possible side chain component)
445 cm^{-1}	na	+	na	na	na	Beta-sheet
520 cm^{-1}	480 or 560 cm^{-1}	+	+?	+?	–	Amide VI (possible side chain component)

400 cm^{-1} correspond with the three actual bands in this region and the simulated band at ~560 cm^{-1} corresponds to the actual band at 520 cm^{-1}. The simulated band at 480 cm^{-1} does not seem to correspond to any band in the experimental data and is probably an artefact of the simulation. The simulation does not account for the underlying baseline shift which is seen as a dome in the data between 50 and 350 cm^{-1}, and the subsequent rise in baseline after 400 cm^{-1}. The intensities of the bands in the simulated IR spectrum were not particularly close to the experimental data.

3.3. Simulation of the peptide AK17's vibrational density of states

The vibrational density of states (VDOS) represents all vibrational modes including those that are infrared inactive so it does not substitute for an IR spectra. While a VDOS spectrum is clearly different from an IR spectrum, VDOS are an important aid to interpret and assign vibrational modes which are observed in the IR spectra [30]. In this paper we used VDOS to distinguish which vibrational modes are associated with the peptide backbone and the side chain, and to determine which modes are associated with hydrogen atoms.

The VDOS simulation of the carbon (C), nitrogen (N) and oxygen (O) atoms of the peptide AK17 backbone (Fig. 4a) gave a complicated series of possible vibrational modes between 0 and 200 cm^{-1} including modes at 100 and 200 cm^{-1} which correspond with modes in the IR simulation. The noise in this part of the simulation could represent diverse vibrational modes at this low wave numbers that may or may not be IR active. The band at 100 cm^{-1} could be interpreted as being associated with either the peptide backbone or the side chain as there are peaks in both simulations but it was not associated with hydrogen. The mode at 200 cm^{-1} was seen in the VDOS simulation of the backbone when only hydrogen was included in the simulation (Fig. 4b). The mode seen at 265 cm^{-1} in the IR simulation was not apparent in the VDOS simulation. The mode at 333 cm^{-1} was apparent in the backbone simulation only and was not associated with hydrogen. The mode at 375 cm^{-1} could be associated with either the peptide backbone or the side chain as there are peaks in both simulations and is not associated with hydrogen. The artefact in the IR simulation at 480 cm^{-1} was not observed in the VDOS simulation. The mode at 580 cm^{-1} could be associated with either the peptide backbone or the side chain as there are peaks in both simulations and was not associated with hydrogen.

3.4. Interpretation of AK17's spectrum

The peak seen in all three spectra for the peptides AK17, AK10G and AK9P at 120 cm^{-1} was unique in its blue shift as the temperature was reduced. This was not observed for the peaks or shoulders at higher wave numbers. This phenomenon has been observed in crystalline lattices where it was attributed to temperature dependant dimensional change in the crystal structure [31]. In the case of these peptides it is possible that the blue-shift phenomenon is also associated with intermolecular interactions. The VDOS simulation indicates that this mode does not involve hydrogen so intermolecular and intramolecular hydrogen bonding is not being observed. A similar peak at 120 cm^{-1} was observed in experimental data of partially hydrated lysozyme and was attributed to protein backbone-solvent hydrogen bonds [32] but the VDOS presented here suggests this is not happening in lyophilized peptide. The VDOS simulation indicated that the vibrational modes at 120 cm^{-1} could be due to peptide backbone or the side chains so there may be more than one cause behind the absorbance at this wave number.

The absorbance maximum at 195 cm^{-1} is possibly the position of a weak band though this is difficult to distinguish in the experimental data. There is a broad band between 50 and 350 cm^{-1}, with a maximum around 200 cm^{-1}, which may correlate to this band in the simulated IR spectrum and the VDOS. Previous researchers have assigned this broad band in experimental data to an ensemble of intramolecular hydrogen bonds [11]. The VDOS suggests that this vibrational mode is associated with hydrogen and is associated with the peptide backbone. The hydrogen bond populations present in α-helices and β-pleated sheets (of AK17 and AK9P, respectively) are quite different and may account for the difference in shape of this broad band (Fig. 1a and c). Research on N-methylacetamine suggested this mode may be due to C—N torsional vibrations [2] but our VDOS simulation would suggest this is

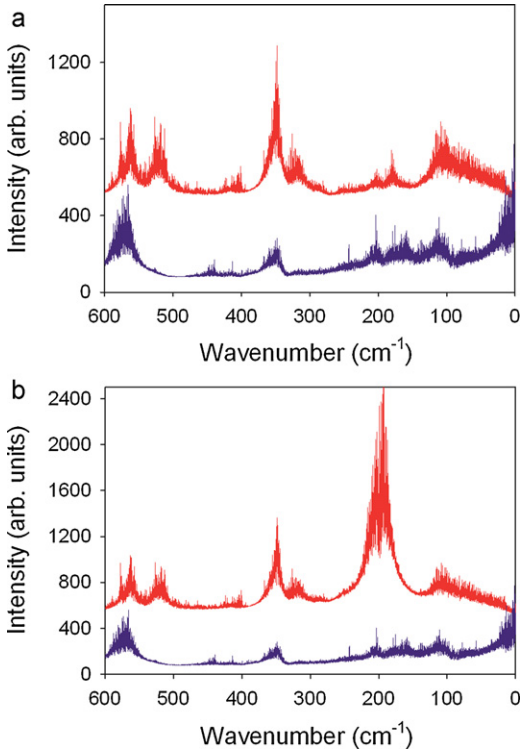

Fig. 4. Vibrational density of states simulation (0–600 cm^{-1}) of AK17 carbon, nitrogen and oxygen without hydrogen (a) backbone (red), side chains (blue) and (b) hydrogen, carbon, nitrogen and oxygen backbone (red), side chains (blue). Side chain and backbone simulations are offset vertically by 400 units for clarity. (For interpretation of the references to color in this figure legend, the reader is referred to the web version of the article.)

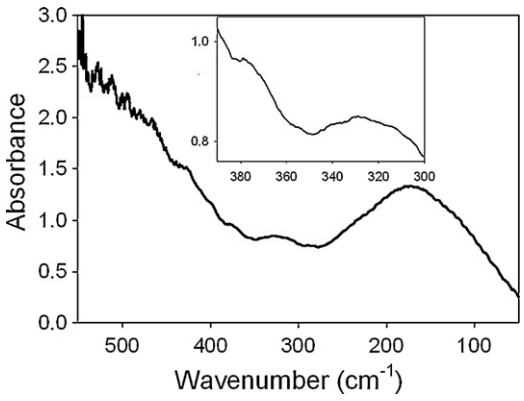

Fig. 5. Experimental far-infrared spectra (50–550 cm^{-1}) of lyophilized lysozyme at 78 K. Inset highlights the peaks at approximately 333 and 380 cm^{-1}.

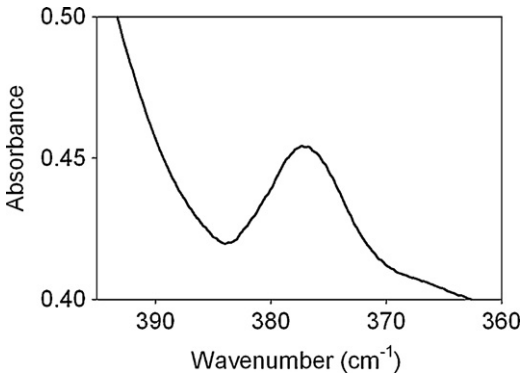

Fig. 6. Experimental far-infrared spectra (360–400 cm^{-1}) of frozen aqueous lysozyme at 78 K.

not the case. The alternative N—H out-of-plane bending [2] is consistent with the VDOS results and may contribute to this feature. The unclear experimental data and the noise in the VDOS simulation around 200 cm^{-1} make any definite conclusion about a mode at 200 cm^{-1} difficult but it does not disprove the theory that it is associated with an ensemble of diverse hydrogen bonds.

The peak at 265 cm^{-1} is present in all three peptides. This peak is reproduced in the simulated IR spectrum but not obvious in the VDOS. Assignment to N—H out-of-plane bending [20] and the CNC deformation [2] is possible. The lack of a vibrational mode at this wave number in the VDOS simulation currently prevents assignment of this band.

The peaks at 333 and 375 cm^{-1} are consistent with those observed in frozen aqueous samples [20]. The disappearance of peak 375 cm^{-1} in the AK9P spectrum is consistent with this vibrational mode being in the peptide backbone and is lost in the switch from α-helix to β-pleated sheet formation. The emergence of a peak at 445 cm^{-1} in the AK9P spectrum is due to the presence of β-sheets. This finding is not unique. A similar phenomenon has been observed for copolymers of L-alanine and L-valine where the addition of dichloroacetic acid can switch the copolymers from an alpha-helix to a beta-sheet conformation. This was accompanied by a peak at 375 cm^{-1} associated with helical form and a peak at 440–443 cm^{-1} associated with the beta-sheet form [4]. The findings are consistent with this part of the infrared spectrum being diagnostic for peptide secondary structure.

The band at approximately 520 cm^{-1} can be identified with the amide VI band attributed to the bending motion of the C=O group in the peptide backbone [6]. This band was observed at 560 cm^{-1} in the simulated IR spectrum but corresponded closely with the 520 cm^{-1} band in the VDOS simulation which was only observed in the VDOS of the peptide backbone and was not associated with hydrogen which is consistent with it being the bending motion of the C=O group. The position of the amide VI maxima did not shift as previously observed [6].

3.5. Optical analysis of lysozyme using far-infrared spectroscopy

To establish whether the findings from experimental and simulation work undertaken with alanine-rich peptides can be transferred to larger globular proteins we undertook analysis of lysozyme both as lyophilized power and as frozen aqueous samples. The spectrum of lyophilized lysozyme had a broad peak centred on 180 cm^{-1}, lying between 50 and 280 cm^{-1}. There is a second minor peak centred at 333 cm^{-1}, another smaller peak on 378 cm^{-1} and a rise in absorbance after 350 cm^{-1} (Fig. 5). This has been observed previously by Buontempo [5]. Preparation of 8% (w/v) lysozyme in an aqueous solution that was frozen to 78 K provided better resolution of the peak at 378 cm^{-1} than seen for the lyophilized sample (Fig. 6). The peak at 380 cm^{-1} for 50 mM AK17 solution in shown in Fig. 5b for comparison purposes.

The very broad peak in absorbance centred on 180 cm^{-1} did not show any discrete peaks but was composed of a relatively smooth regular broad peak between 50 and 300 cm^{-1}. This may be partially due to a population of overlapping discrete vibrational modes associated with hydrogen bond formation that swamp out the discrete vibrational modes seen in the peptide spectra. Of the discrete vibrational modes still observable in the lysozyme spectrum is the shoulder seen between 360 and 385 cm^{-1} which likely corresponds to the 375 cm^{-1} peak observed in the AK17 spectrum that was associated with the alpha-helical backbone vibrational modes. Lysozyme, like AK17, is rich in alpha-helices in its native state [33]. The peak at 375 cm^{-1} is much clearer in frozen aqueous samples (Fig. 6) rather than lyophilized protein samples (Fig. 5) and can be observed for both lysozyme and AK17 samples. This finding suggests that the frozen thin sample may be preferable to lyophilization in studying the secondary structure of both peptides and small proteins.

3.6. Optical analysis of non-cyclic and cyclic peptides using far-infrared spectroscopy

The pentameric peptide with the amino acid sequence KARAD in its non-cyclic form and cyclized by formation of a peptide bond between the first residue (lysine) and the fifth residue (aspartate) [34] were analysed as frozen aqueous samples at 78 K as previously described which limits the usable bandwidth from 300 to 550 cm^{-1} [20]. The non-cyclic KARAD had a spectrum with minor shifts in the baseline and a significant peak at 530 cm^{-1} (Fig. 7). The cyclized peptide (with a strong helical structure) spectrum was radically different and had additional peaks at 385, 402 and 470 cm^{-1}.

The presence of bands at 385, 402 and 470 cm^{-1} in the spectrum of cyclized KARAD but not in non-cyclized KARAD indicates that low wave number vibrational modes were detectable in the strongly helical cyclic peptide [34] but were absent in the non-cyclic peptide with exactly the same amino acid sequence. This observation supports the finding of a strong link between secondary structure of peptides and the presence of distinct vibrational modes between 300 and 500 cm^{-1}. It also suggests that low wave number vibrational modes in these strongly helical cyclic peptides were measurably different to the alpha helices in non-cyclic helical peptides like AK17. Again this suggests that the frozen thin samples are suitable for studying the secondary structure of peptides.

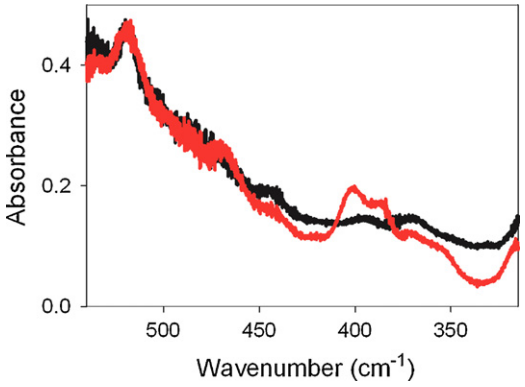

Fig. 7. Experimental far-infrared spectra (315–540 cm^{-1}) of frozen aqueous KARAD peptides measured at 78 K, relative to buffer. Non-cyclic (black) and cyclic (red) KARAD. (For interpretation of the references to color in this figure legend, the reader is referred to the web version of the article.)

4. Conclusions

The nature of the information captured by far-infra red spectroscopy of polypeptides at wave number values below 300 cm^{-1} is dependent on the molecular weight of the molecule. The simplest molecule containing a peptide bond (N-methylacetamide) has only two discrete bands at 120 and 201 cm^{-1} in the liquid state which can be assigned to specific vibrational modes (CO···HN hydrogen bonding and C—N torsional vibration, respectively) [1]. For analysis of more complex peptides (in our case alanine-rich peptides composed of 17 amino acid residues), the number of discrete vibrational modes increases as seen in the peaks centred at 120, 195, 265, 333, 375, 445 and 520 cm^{-1} (375 cm^{-1} in peptides with alpha-helices and 445 cm^{-1} in peptide with beta-pleated sheets). There is also a shift in the baseline between 50 and 300 cm^{-1} indicating that there is a broad peak that is due to an ensemble of vibrational modes with discrete vibrational modes emerging from this broad feature. For analysis of larger molecules such as lysozyme with 129 amino acid residues, a broad peak is observed centred around 180 cm^{-1}. This broad peak again is due to an ensemble of vibrational modes possibly dominated by hydrogen bond vibrational modes that swamp the discrete vibrational modes seen in peptide spectra, with the exception of the peak at 375 cm^{-1}, which is associated with the high alpha-helix component of lysozyme's backbone. The hypothesis that the broad feature between 50 and 300 cm^{-1} is due to intramolecular hydrogen bonds [35] is contradicted by earlier work where lysozyme was heat treated and allowed to assemble in fibrils where there was a lack of change in the broad peak even after radical changes to the secondary structure of the protein [14]. The feature may well be due to structural collective motions within the protein, a theory that has been supported by VDOS simulation of these modes and has been suggested to explain the spectrum observed using THz-TDS between 2 and 90 cm^{-1} [36]. Supporting both theories, the change in the population of intramolecular hydrogen bonds and the structural collective motions are consistent with the changes observed in the spectra below 300 cm^{-1} as the molecular weight of the peptide/protein increases from 73 Da for N-methylacetamide to 1482 Da for AK17 to 14,388 Da for lysozyme.

Where far-infrared spectroscopy does provide valuable information for peptides and possibly small proteins is for the wave number range 300–500 cm^{-1}, where there is evidence that low wave number vibrational modes are related to secondary structure. The presence of bands at 333 and 380 cm^{-1} associated with alpha-helix structures in non-cyclic AK17 peptide (confirmed by circular dichroism spectroscopy),[17] the band at 445 cm^{-1} associated with beta-pleated sheet formation in AK9P (confirmed by Raman spectroscopy of the amide I band) and the bands at 385, 402 and 470 cm^{-1} associated with the strongly helical cyclic structure of cyclo-KARAD (confirmed by circular dichroism spectroscopy),[29] supports the hypothesis that vibrational modes in this wave number range relate to the secondary structure of peptides. While the work presented here used a synchrotron light source and liquid helium cooled bolometer, other methodologies have been successfully applied to study proteins at these wave numbers including FTIR with an ATR diamond prism [35] and FTIR in transmission mode using very thin samples, liquid helium cooled bolometer and a traditional light source [30]. Both of these methods are amenable to routine use in laboratories.

Acknowledgements

This work was funded by the Australian Research Council grant numbers DP0773111 and DP1093056. TH thanks the Australian Research Council for a Future Fellowship. AM thanks the Government of Queenlsand for a fellowship under the Smart Futures scheme. We thank the Australian Synchrotron for access to their infrared beam-line, Dominique Appadoo and Danielle Martin for their assistance, Bill van Bronswijk for the PE powder and David Fairlie for the KARAD peptides.

References

[1] K. Itoh, T. Shimanouchi, Biopolymers 5 (1965) 921.
[2] J. Bandekar, Biochim. Biophys. Acta 1120 (1992) 123.
[3] W.H. Moore, S. Krimm, Biopolymers 15 (1976) 2465.
[4] K. Itoh, H. Katabuchi, Biopolymers 12 (1973) 921.
[5] U. Buontempo, C. Careri, P. Fasella, A. Ferraro, Biopolymers 10 (1971) 2377.
[6] Y. El Khoury, R. Hielscher, M. Voisecu, J. Gross, P. Hellwig, Vib. Spectrosc. 55 (2011) 258–266.
[7] A.G. Markelz, A. Roitberg, E.J. Heilweil, Chem. Phys. Lett. 320 (2000) 42–48.
[8] B.M. Fischer, M. Walther, P.U. Jepsen, Phys. Med. Biol. 47 (2002) 3807.
[9] A.G. Markelz, J.R. Knab, J.Y. Chen, Y.F. He, Chem. Phys. Lett. 442 (2007) 413–417.
[10] Y.F. He, J.Y. Chen, J.R. Knab, W. Zheng, A.G. Markelz, Biophys. J. 100 (2011) 1058–1065.
[11] Y. El Khoury, A. Trivella, J. Gross, P. Hellwig, ChemPhysChem 12 (2011) 217–224.
[12] S. Ebbinghaus, S.J. Kim, M. Heyden, X. Yu, U. Heugen, M. Gruebele, D.M. Leitner, M. Havenith, Proc. Natl. Acad. Sci. U.S.A. 104 (2007) 20749–20752.
[13] G. Png, R.J. Falconer, B.M. Fischer, H.A. Zakaria, S. Mickan, A.P.J. Middelberg, D. Abbott, Opt. Express 17 (2009) 13102–13115.
[14] H. Zakaria, I. Jones, B.M. Fischer, D. Abbott, A.P.J. Middelberg, R.J. Falconer, Appl. Spectrosc. 65 (2011) 260–264.
[15] R.J. Falconer, H. Zakaria, Y.Y. Fan, A.P. Bradley, A.P.J. Middelberg, Appl. Spectrosc. 64 (2010) 1259–1264.
[16] H. Born, E. Weingartner, E. Brundermann, M. Havenith, J. Am. Chem. Soc. 131 (2009) 3752–3755.
[17] T. Ding, R. Li, J.A. Zeitler, T.L. Huber, L.F. Gladden, A.P.J. Middelberg, R.J. Falconer, Opt. Express 18 (2010) 27431–27444.
[18] J.B. Brubach, A. Mermet, A. Filabozzi, A. Gershel, P. Roy, J. Chem. Phys. 122 (2005) 122.
[19] W. Wang, Int. J. Pharm. 203 (2000) 1–60.
[20] T. Ding, T. Huber, A.P.J. Middelberg, R.J. Falconer, J. Phys. Chem. A 115 (2011) 11559–11565.
[21] N.J. Greenfield, S.E. Hitchcock-Degregori, Protein Sci. 2 (1993) 1263–1273.
[22] N. Eswar, B. Webb, M.A. Marti-Renom, M.S. Madhusudhan, D. Eramian, M.-Y. Shen, U. Pieper, A. Sali, Unit 2.9. Comparative Protein Structure Modeling Using MODELLER, Wiley, Hoboken, 2007.
[23] H.J.C. Berendsen, J.P.M. Postma, W.F. van Gunsteren, J. Hermans, in: B. Pullman (Ed.), Intermolecular Forces, D. Reidel Publishing Company, Dordrecht, 1981, pp. 331–342.
[24] L.D. Schuler, X. Daura, W.F. Van Gunsteren, J. Comput. Chem. 22 (2001) 1205–1218.
[25] D.A. McQuarrie, Statistical Mechanics, New York, Harper-Collins Publishers, 1976.
[26] P.H. Berens, D.H. Mackay, G.M. White, K.R. Wilson, J. Chem. Phys. 79 (1983) 2375–2389.
[27] J.J. Schwegman, J.F. Carpenter, S.L. Nail, J. Pharm. Sci. 96 (1969) 179–195.
[28] N.T. Yu, C.S. Liu, D.C. O'Shea, J. Mol. Biol. 70 (1972) 117–132.
[29] T.G. Spiro, B.P. Gaber, Ann. Rev. Biochem. 46 (1977) 553–572.
[30] M.P. Gaigeot, M. Martinez, R. Vuilleumier, Mol. Phys. 105 (2007) 2857–2878.

[31] B.M. Fischer, H. Helm, P.U. Jepsen, Proc. IEEE 95 (2007) 1592–1604.
[32] K.N. Woods, Phys. Rev. E 81 (2010) 031915.
[33] N.E. Shepherd, H.N. Hoang, G. Abbenante, D.P. Fairlie, J. Am. Chem. Soc. 127 (2005) 2974–2983.
[34] S.W. Provencher, J. Glockner, Biochemistry-US 20 (1981) 33–37.
[35] R. Hielscher, T. Friedrich, P. Hellwig, ChemPhysChem 12 (2011) 217–224.
[36] Y.F. He, J.Y. Chen, J.R. Knab, W.J. Zheng, A.G. Markelz, Biophys. J. 100 (2011) 1058–1065.